Minimally adhesive polymer surfaces (MAPS) prepared from star oligosiloxanes and star oligofluorosiloxanes

ARTICLE *in* JOURNAL OF POLYMER SCIENCE PART A POLYMER CHEMISTRY · APRIL 2006

Impact Factor: 3.11 · DOI: 10.1002/pola.21362

8 AUTHORS, INCLUDING:

Melissa A Grunlan
Texas A&M University
56 PUBLICATIONS **615** CITATIONS
SEE PROFILE

Florian Mansfeld
University of Southern California
325 PUBLICATIONS **8,229** CITATIONS
SEE PROFILE

Minimally Adhesive Polymer Surfaces Prepared from Star Oligosiloxanes and Star Oligofluorosiloxanes

MELISSA A. GRUNLAN,[1] NAM S. LEE,[1] FLORIAN MANSFELD,[2] ESRA KUS,[2] JOHN A. FINLAY,[3] JAMES A. CALLOW,[3] MAUREEN E. CALLOW,[3] WILLIAM P. WEBER[1]

[1]Loker Hydrocarbon Research Institute, Department of Chemistry, University of Southern California, Los Angeles, California 90089-1661

[2]Material Science and Engineering, University of Southern California, Los Angeles, California 90089-1661

[3]School of Biosciences, University of Birmingham, Birmingham, B15 2TT, England

Received 3 June 2005; accepted 30 January 2006
DOI: 10.1002/pola.21362
Published online in Wiley InterScience (www.interscience.wiley.com).

ABSTRACT: The effects of the surface energy, storage modulus (G'), and glass-transition temperature (T_g) on the biofouling behavior of siloxane and fluorosiloxane polymer surfaces (films) were studied. Irregular Si—H-terminated tetrabranched star oligosiloxanes and star oligofluorosiloxanes were prepared by the acid-catalyzed equilibration of octamethylcyclotetrasiloxane or 1,3,5-trimethyl-1,3,5-tris(3′,3′,3′-trifluoropropyl)cyclotrisiloxane with tetrakis(dimethylsiloxy)silane, respectively. Terminal epoxy groups were introduced via Pt-catalyzed hydrosilylation with allyl glycidyl ether to yield compounds that were subsequently crosslinked with α,ω-bis(3-aminopropyl)poly(dimethylsiloxane). The resulting films were characterized by goniometry, dynamic mechanical thermal analysis, and thermogravimetric analysis. The foul-release behavior was studied by the measurement of how strongly sporelings (young plants) of the green seaweed *Ulva* adhered. The corrosion protection of aluminum was evaluated by electrochemical impedance spectroscopy. Fluorosiloxane films displayed higher G' and T_g values, decreased contact angles (with water), and more effectively released *Ulva* sporelings in comparison with siloxane films. © 2006 Wiley Periodicals, Inc. J Polym Sci Part A: Polym Chem 44: 2551–2566, 2006

Keywords: films; fluoropolymers; polysiloxanes; star polymers

INTRODUCTION

There is interest in noninteractive minimally adhesive polymer surfaces (MAPSs), which resist adhesion.[1,2] For marine coatings, the ability of polymer surfaces to minimize the attachment of organisms (i.e., biofoulers) is valuable.[3,4] Traditional antifouling coatings leach nonspecific toxicants such as tributyl tin (TBT), copper, or organic biocides.[4] However, their accumulation and negative impact on nontarget marine life has prompted an international ban of TBT and restrictions on copper.[5] Thus, MAPSs are promising candidates for nontoxic foul-release coatings from which biofoulers may be removed by hydrodynamic self-cleaning or by a water jet.[6]

Most MAPSs are prepared from siloxanes,[2,7–10] fluoropolymers,[11–14] and fluorosiloxanes.[15–18] Their nonadhesive nature is attributed to (1) low surface energies (γ), (2) low storage moduli (G'), and (3) low glass-transition temperatures (T_g's).[19] Low γ values reduce polar and hydrogen-bonding interactions with the marine organism's adhesive, thereby

Correspondence to: W. P. Weber (E-mail: wpweber@usc.edu)

Journal of Polymer Science: Part A: Polymer Chemistry, Vol. 44, 2551–2566 (2006)

decreasing the joint strength.[6] However, G' is also significant because the rupture of an adhesive bond involves viscoelastic flow at the coating surface.[20] The force required to remove rigid solids adhering to elastomers on rigid substrates is proportional to $(G'\gamma)^{1/2}$.[21] The removal of viscoelastic adhesives occurs more readily from siloxanes than fluorosiloxanes, despite the latter's lower γ value.[22] The lower G' value of the siloxane enhances interfacial slippage and decreases adhesion. A reduction in adhesion to a siloxane coating has been attributed to a decrease in G' upon the depletion of its $CaCO_3$ filler.[23] Finally, low-T_g materials produce surfaces with high molecular mobility, which may inhibit permanent bond formation.[4] Thus, the flexibility of the siloxane backbone mobilizes pendant functional groups, preventing compatible groups of the adhesive from locating and binding to them.[24]

Designing MAPSs requires the selection of appropriate precursors, crosslinkers, and cure chemistry to produce films with desired properties. In this study, films were formed from both linear siloxanes (**a**–**c**) and star oligosiloxanes (**III** and **VII**) or star oligofluorosiloxanes (**IV** and **VIII**). Branched or star polymers are of interest as they may exhibit distinct properties versus linear analogues.[25–28] End-functionalized branched polymers may act as crosslinkers and limit the phase separation of components, thereby improving the film strength.[28] The film composition was controlled by the incorporation of either star oligosiloxanes or star oligofluorosiloxanes. The γ value of a fluorosiloxane is generally lower than that of a similar siloxane.[29] The crosslink density was controlled by the variation of the molecular weights of linear siloxanes (**a**–**c**) and star oligosiloxanes (**III** and **VII**) or star oligofluorosiloxanes (**IV** and **VIII**). Crosslinkable epoxy groups were introduced by the Pt-catalyzed hydrosilylation of allyl glycidyl ether and Si—H moieties of tetrakis(ω-dimethylsiloxy)oligo(dimethylsiloxy)silane (**I**), tetrakis(dimethylsiloxy) oligo[3′,3′,3′-trifluoropropylmethylsiloxy]silane (**II**), **V**, and **VI**.[28,30] Epoxy-terminated siloxanes have been crosslinked with a UV photoacid catalyst.[15,31–33] However, in this study, epoxy groups of **III**, **IV**, **VII**, and **VIII** were thermally cured with primary aliphatic amines (**a**–**c**).[34]

Synthetic Approach

Here we report the preparation of siloxane (**IIIa**–**IIIc** and **VIIa**–**VIIc**) and fluorosiloxane films (**IVa**, **IVb**, **VIIIa**, and **VIIIb**) prepared by the crosslinking of ω-epoxy tetrabranched star oligosiloxanes (**III** and **VII**) or star oligofluorosiloxanes (**IV** and **VIII**) with an α,ω-bis(3-aminopropyl)poly(dimethylsiloxane) [α,ω-bis(3-aminopropyl) PDMS; **a**–**c**]. The synthetic sequence consists of (1) the preparation of **I** or **II** by the acid-catalyzed equilibration of octamethylcyclotetrasiloxane (D_4) or 1,3,5-trimethyl-1,3,5-tris(3′,3′,3′-trifluoropropyl)cyclotrisiloxane (D_3^F), respectively, with tetrakis(dimethylsiloxy)silane (tetra-SiH)[31] (the molecular weight was controlled by the ratio of tetra-SiH and D_4 or D_3^F); (2) the optional removal of the lower molecular weight material from **I** or **II** to isolate **V** or **VI**, respectively; (3) the Pt-catalyzed hydrosilylation of **I**, **II**, **V**, or **VI** with allyl glycidyl ether to yield tetrakis[(ω-glycidyloxypropyl)polydimethylsiloxy]silanes (**III** and **VII**) and tetrakis[ω-(dimethylsiloxy)poly(3′,3′,3′-trifluoropropyl)methylsiloxy]silanes (**IV** and **VIII**); and (4) finally, the thermal cure of **a**, **b**, or **c** with **III**, **IV**, **VII**, or **VIII** to form films of **IIIa**–**IIIc**, **IVa** and **IVb**, **VIIa**–**VIIc**, or **VIIIa** and **VIIIb**. 2,4,6-[Tris(dimethylamino)phenol] catalyzed the formation of siloxane films (**IIIa**–**IIIc** and **VIIa**–**VIIc**), whereas phenol catalyzed the formation of fluorosiloxane films (**IVa**, **IVb**, **VIIIa**, and **VIIIb**). The synthesis of **I**–**VIII** is presented in Figure 1. The film preparation is shown in Figure 2.

Solutions of **III**, **IV**, **VII**, or **VIII**, α,ω-bis(3-aminopropyl)PDMS (**a**, **b**, or **c**), and a catalyst (0.5 wt %) were deposited onto microscope slides or aluminum coupons. These were cured at 115 °C for 24 h. The static contact angles (θ_{static}), as well as the advancing dynamic contact angles (θ_{adv}) and receding dynamic contact angles (θ_{rec}), of distilled/deionized water on the air–film interface were determined by goniometry. T_g and G' values of films were obtained by dynamic mechanical thermal analysis (DMTA), and thermal stabilities were determined by thermogravimetric analysis (TGA). Biofouling was studied by the strength of attachment assays of sporelings (young plants) of *Ulva*. *Ulva* is the most predominant ship-fouling macroalga and has been used extensively as a test organism for laboratory studies of marine coatings designed to resist biofouling.[35,36] Corrosion protection of aluminum (3105 H14 alloy) was studied by electrochemical impedance spectroscopy (EIS).

EXPERIMENTAL

Instrumentation

Polymer Characterization

^1H, ^{13}C, ^{29}Si, and ^{19}F NMR spectra were acquired on a Bruker AMX 500-MHz spectrometer oper-

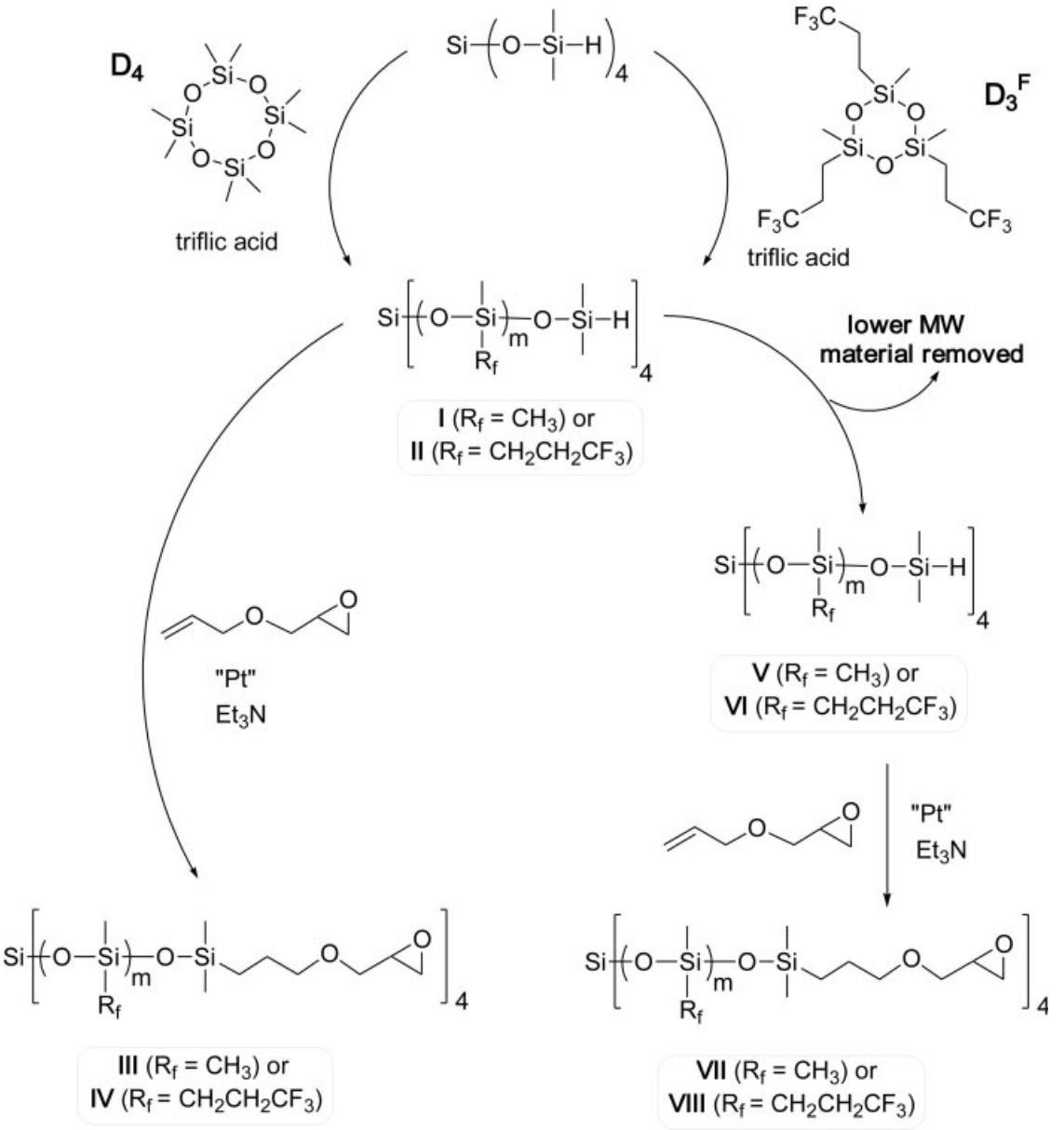

Figure 1. Synthesis of **I**–**VIII**.

ating in the Fourier transform mode. ^{1}H, ^{13}C, and ^{19}F spectra of 5% (w/v) $CDCl_3$ solutions were obtained. ^{29}Si NMR spectra of 25% (w/v) $CDCl_3$ solutions were acquired. ^{13}C NMR spectra were run with broad-band proton decoupling. A heteronuclear gated decoupling pulse sequence (NONOE) with a 60-s delay was used to acquire ^{29}Si NMR spectra. Residual $CDCl_3$ was used as an internal standard for ^{1}H and ^{13}C NMR. ^{19}F NMR spectra were referenced to internal $CFCl_3$. ^{29}Si NMR spectra were referenced to internal tetramethylsilane. Higher molecular weight fluorosiloxanes were not soluble in $CDCl_3$. Their NMR spectra were obtained for neat liquids with a sealed capillary of acetone-d_6. IR spectra of neat liquids on NaCl plates were recorded with a PerkinElmer Spectrum 2000 Fourier transform infrared spectrometer.

Gel permeation chromatography (GPC) analysis of the weight-average molecular weight (M_w) and number-average molecular weight (M_n) was performed on a Waters system equipped with a refractive-index detector and two 7.8 mm $\times$ 300 mm Styragel (HR4 and HR2) columns. The eluting solvent was toluene or tetrahydrofuran at a flow rate of 0.6 mL/min. The retention times were cali-

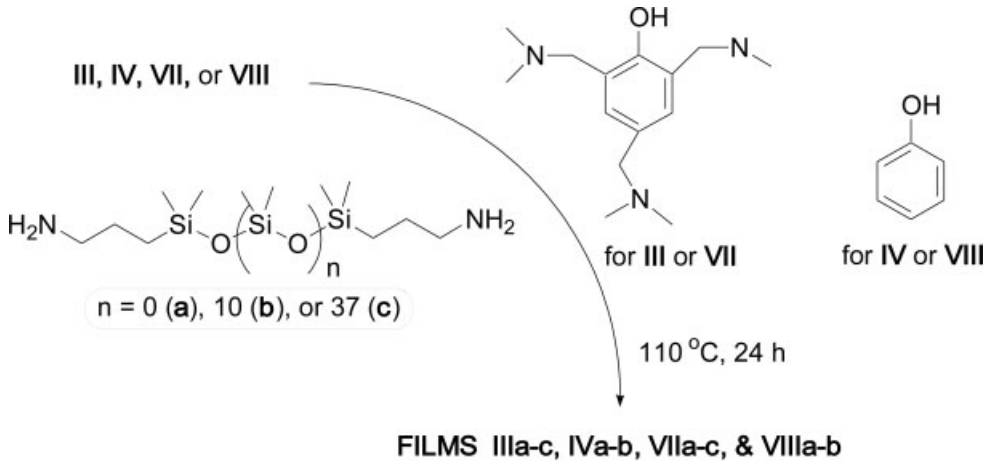

Figure 2. Cure reactions to form siloxane films (**IIIa–IIIc** and **VIIa–VIIc**) and fluorosiloxane films (**IVa**, **IVb**, **VIIIa**, and **VIIIb**).

brated against five known polystyrene standards. The values of M_n are reported directly from monomodal GPC results. For a bimodal GPC result, an average value of M_n was calculated on the basis of the amount of the lower molecular weight material removed by distillation or the weight-loss percentage at low temperatures (TGA, N_2).

TGA was measured on a Shimadzu TGA-50 instrument from 25 to 800 °C (4 °C/min) under 40 cc/min of N_2 or air. T_g's were determined on a Shimadzu DSC-50. The differential scanning calorimeter was calibrated from the thermal transition temperature (−87.06 °C) and melting point (6.54 °C) of cyclohexane.[37] After equilibration at −150 °C for 5 min, the temperature was increased at 10 °C/min to 25 °C.

Film Characterization

T_g and G' values of films were determined by DMTA with a TA Instruments Q800 DMA 5 in the three-point-bending configuration (frequency = 5 Hz). After 4 min at −130 °C, the temperature was increased at 5 °C/min to 30 °C. TGA of free-standing films was obtained in N_2. Electronic calipers were used to measure the film thickness.

θ_{static}, θ_{adv}, and θ_{rec} of distilled/deionized water at the air–film interface were measured with a First Ten Ångstroms 4000 system at 24 °C and 58% relative humidity. θ_{static} of a sessile drop of water (5 μL) was measured 5 s after deposition. Three measurements were performed on each film with a fresh water droplet, and the values were averaged. θ_{adv} and θ_{rec} were similarly measured. A 5-μL pendant droplet of water was initially applied. An additional 2 μL was added at a rate of 1 μL/min to advance the contact line and determine θ_{adv}. θ_{rec} was measured by the subsequent removal of 4 μL from the same drop, which caused the contact line to recede.

Biotesting with Ulva *Sporelings*

Zoospores were released from fertile *Ulva linza* plants and prepared for adhesion experiments.[38] Surface colonization was achieved by the settlement and adhesion of motile spores, which subsequently germinated into sporelings.[38] Twelve replicate coated microscope slides and acid-washed, uncoated controls were tested. Slides were leached first for 4 weeks in stirred deionized water and then in seawater for 1 h before testing. Zoospores were allowed to settle over 4 h.[39] Nonadhered spores were exposed to light to observe their motility and determine leachate toxicity. Adhered spores were cultured for 10 days.[35] The biomass and strength of attachment of the sporelings (young plants) were quantified according to published methods.[35] The sporeling biofilm was scraped from half of each slide into a tube and quantified by the extraction of chlorophyll *a* into dimethyl sulfoxide.[40] The remaining sporelings on the other half of each slide were exposed to a wall shear stress of 53 Pa for 5 min in a turbulent channel flow apparatus.[41,42] The sporeling biomass remaining was estimated by the extraction of chlorophyll *a* as previously discussed. The percentage of biomass removal after exposure to shear was calculated. Error bars were obtained from arcsine transformed data. The significance was tested with a one-way analysis of variance, and when significant differences were found, the

means were compared with Tukey's test. Glass was included in the assays as a standard.

Evaluation of Corrosion Protection with EIS

The corrosion behavior of coated aluminum (3105 H14 alloy) panels was evaluated in a 0.5 N NaCl solution (open to air) at room temperature. EIS measurements were obtained at the open-circuit or corrosion potential in the frequency range of 100 KHz to 5 mHz with a Gamry PCI4/300 potentiostat and Gamry EIS300 software. A stainless steel counter electrode and a saturated calomel reference electrode were used for the measurements. The samples were exposed to the test solution for ~30 days, and measurements were taken as a function of time. The exposed area was 5 cm^2. The impedance spectra are displayed as Bode plots, in which the logarithm of the impedance modulus and the phase angle are shown as functions of the logarithm of the frequency of the applied signal (shown later in Fig. 8).

Materials

D_4, D_3^F, tetra-SiH, α,ω-bis(3-aminopropyl)PDMS [M_n = 1000 (**b**) or 3000 (**c**)] and 1,3-bis(aminopropyl)tetramethyldisiloxane (**a**), and the Pt–divinyltetramethyldisiloxane complex (Karstedt's catalyst) in xylene (2% Pt) were acquired from Gelest. Triflic acid, triethylamine (Et_3N), $MgCO_3$, allyl glycidyl ether, 2,4,6-tris(dimethylamino)phenol, and phenol were received from Aldrich. Q-Panel type A (3105 H14 alloy; ASTM B 209M) aluminum panels (3.0″ × 5.0″ × 0.025″) were from Gardner Co.

General Synthetic Procedure

I or **II** was prepared by the combination of D_4 (for **I**) or D_3^F (for **II**) and tetra-SiH in a 500-mL, round-bottom (rb) flask equipped with a Teflon-covered magnetic stirring bar and sealed with a rubber septum. The vessel was purged with N_2, and triflic acid was added. The mixture was allowed to stir for 1 h at 90 °C (for **I**) or for 24 h at 50 °C (for **II**). After it cooled, a slurry of $MgCO_3$ and CH_2Cl_2 was added, the mixture was stirred for 2 h and filtered through a pad of Celite, and volatiles were removed by evaporation under reduced pressure.

Pt-catalyzed hydrosilylation reactions were performed as follows. **I**, **II**, **V**, or **VI** was combined with Et_3N and 75% of Karstedt's catalyst in a 500-mL, rb flask as above. Allyl glycidyl ether was added over 30 min, and the remaining Karstedt's catalyst added. The mixture was stirred at 75 °C overnight (under N_2) and cooled, and excess allyl glycidyl ether was removed by distillation. The residue was purified by flash column chromatography on silica gel with hexanes/CH_2Cl_2 (4/1). Volatiles were removed under reduced pressure.

Film Preparation

In a 25-mL, rb flask equipped with a Teflon-covered magnetic stirring bar, **III**, **IV**, **VII**, or **VIII** (~10 g) was combined with **a**, **b**, or **c** (50% molar ratio of amino groups to glycidyloxy moieties) and stirred for ~10 min. The catalyst (0.5 wt %) 2,4,6-tris(dimethylamino)phenol (for **III** and **VII**) or phenol (for **IV** and **VIII**) was added, and the mixture was stirred for 30 min.

Microscope slides were sequentially cleaned with acetone and CH_2Cl_2 (50/50 v/v), dried in an oven (100 °C), and flame-dried before coating. The aforementioned mixture (1.2 mL) was deposited onto a slide and allowed to level so as to cover the entire slide. Coated slides were placed in a 115 °C oven for 24 h. Films were removed with a clean single-edge razor for DMTA and TGA but remained attached to slides for contact-angle analysis.

Aluminum coupons were cleaned as previously stated and dried overnight at 100 °C. One milliliter of the mixture was applied to a 3″ × 2″ section of an aluminum panel. The liquid was allowed to level before being placed in a level 115 °C oven for 24 h.

Synthesis of I (M_n = 2800 g/mol)

D_4 (200 g, 0.67 mol), tetra-SiH (13 g, 0.04 mol), and triflic acid (100 μL) were reacted as above. A clear, colorless liquid [205.7 g, 97% yield, T_g = −127 °C, M_w/M_n (bimodal) = 6710/3035 and 410/390 g/mol] was obtained.

^{1}H NMR (δ): 0.22 (m, 404H), 0.33 (d, 24H, J = 2.5 Hz), 4.55 (septet, 4H, J = 3 Hz) ppm. ^{13}C NMR (δ): 1.07 ppm. ^{29}Si NMR (δ): [−21.95, −21.84, −21.57, −19.92, −19.17, −18.54] 77Si, −6.97 (m, 4Si) ppm. IR (ν): 2127 (Si—H) cm^{-1}.

For TGA (N_2), see Figure 3. In TGA (air), **I** lost ~9% of its weight below 175 °C. Between 200 and 550 °C, an additional 40% weight loss occurred. **I** contained ~9% material with M_n = 390 g/mol and ~91% material with M_n = 3035 g/mol (see **V** later). This gave an average M_n value of 2800 g/mol.

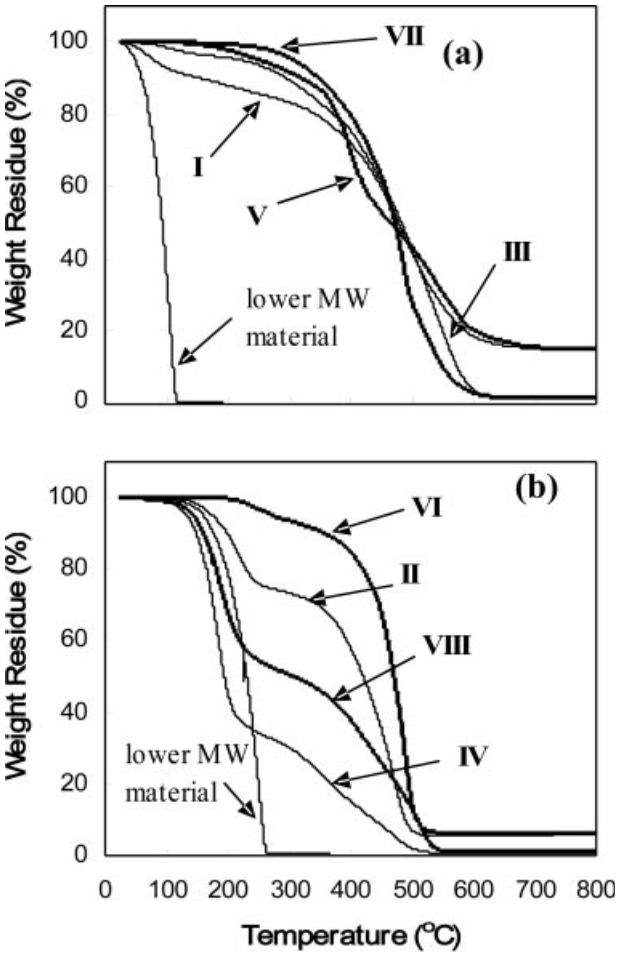

Figure 3. TGA (N_2) for (a) **I** (M_n = 2800 g/mol), corresponding **III**, **V**, and **VII**, and lower molecular weight material removed from **I** and (b) **II** (M_n = 5780 g/mol), corresponding **IV**, **VI**, and **VIII**, and lower molecular weight material removed from **II**.

Synthesis of III (M_n = 3265 g/mol)

I (199.7 g, M_n = 2800 g/mol), Et_3N (150 μL), Karstedt's catalyst (100 μL), and allyl glycidyl ether (63 mL, 0.53 mol) were reacted as above. **III** [189.7 g, 75% yield, T_g = −119 °C, M_w/M_n (bimodal) = 6310/3400 and 725/690 g/mol] was obtained.

^{1}H NMR (δ): [−0.21 (s), −0.12 (s), −0.91 (s), −0.067 (s), 0.026 (s)] 454H, 0.38 (t, 8H, J = 8.5 Hz), 1.45 (m, 8H), 2.45 (dd, 4H, J = 4.5 and 2.5 Hz), 2.63 (t, 4H, J = 4 Hz), 2.98 (m, 4H), 3.23 (dd, 4H, J = 6.0 and 5.5 Hz), 3.29 (m, 8H), 3.54 (dd, 4H, J = 8.0 and 3.0 Hz) ppm. ^{13}C NMR (δ): 0.91, 1.12, 14.23, 23.56, 44.41, 50.96, 71.53, 74.45 ppm. ^{29}Si NMR (δ): [−22.23, −22.10, −21.74, −21–58, −19.35, −18.67] 127Si; 7.54 (s, 4Si) ppm. IR (ν): no Si—H band.

For TGA (N_2), see Figure 3. In TGA (air), **III** lost ~10% of its weight below 175 °C and 50% between 200 and 500 °C. On the basis of GPC and TGA (N_2) results, **III** contained ~5% material with M_n = 690 g/mol and ~95% material with M_n = 3400 g/mol. This gave an average M_n value of 3265 g/mol.

Preparation of V (M_n = 3700 g/mol)

Lower molecular weight material (8.0 g or 9%) was removed from **I** (M_n = 2800 g/mol, 91.4 g) via bulb-to-bulb distillation at 100 °C/0.005 mm to give the higher molecular weight material **V** (83.1 g, T_g = −127 °C, M_w/M_n = 7840/3700 g/mol).

^{1}H NMR (δ): [−0.07 (s), −0.04 (s)] 530H, 0.039 (m, 34H), 4.57 (m, 4H) ppm. ^{13}C NMR (δ): 1.15 ppm. ^{29}Si NMR (δ): [−22.70, −21.90, −21.86, −21.78, −21.34, −19.85, −18.94, −18.50] 69Si; 6.88 (m, 4Si) ppm. IR (ν): 2128 (Si—H) cm^{-1}.

For TGA (N_2), see Figure 3. In TGA (air), **V** lost 60% of its weight between 200 and 500 °C. The lower molecular weight material removed from **I** (M_n = 2800 g/mol] had T_g = −128 °C and M_w/M_n = 410/370 g/mol.

IR (ν): 2127 (Si—H) cm^{-1}.

Synthesis of VII (M_n = 3600 g/mol)

V (80.6 g, M_n = 3700 g/mol), Et_3N (60 μL), Karstedt's catalyst (40 μL), and allyl glycidyl ether (31.6 mL, 0.27 mol) were reacted as above. Thus, **VII** (90.0 g, 81% yield, T_g = −118 °C, M_w/M_n = 7990/3600 g/mol) was obtained.

^{1}H NMR (δ): [−0.21 (s), −0.11 (s), −0.90 (s), −0.064 (s), 0.028 (s)] 455H; 0.38 (t, 8H, J = 8.5 Hz), 1.46 (m, 9H), 2.45 (m, 4H), 2.64 (m, 4H), 3.00 (m, 3H), 3.23 (dd, 4H, J = 6.0 and 5.0), 3.29 (m, 8H), 3.54 (dd, 4H, J = 9.0 and 3.0 Hz) ppm. ^{13}C NMR (δ): 0.17, 1.11, 14.21, 23.54, 44.43 (m), 50.96, 71.51, 74.44 ppm. ^{29}Si NMR (δ): [−22.14, −22.01, −21.74, −21.47, −18.59] 90Si; 7.59 (s, 4Si) ppm. IR (ν): no Si—H band.

For TGA (N_2), see Figure 3. In TGA (air), **VII** lost 55% of its weight from 200 to 550 °C.

Synthesis of I (M_n = 1260 g/mol)

D_4 (150 g, 0.51 mol), tetra-SiH (22.14 g, 0.07 mol), and triflic acid (75 μL) were reacted as above. **I** (166.8 g, 97% yield, T_g = −130 °C, M_w/M_n = 3100/1260 g/mol) was obtained.

^{1}H NMR (δ): [−0.066 (s), −0.055 (s), −0.047 (s), −0.023 (m)] 284H, 0.048 (d, 24H, J = 3 Hz) ppm.

^{13}C NMR (δ): 1.23 ppm. ^{29}Si NMR (δ): [−21.98, −21.94, −21.88, −21.61, −21.38, −19.96, −19.21, −18.56] 40Si, −6.98 (m, 4Si) ppm. IR (ν): 2129 (Si—H) cm^{-1}.

In TGA (N_2 and air), **I** lost ~20% of its weight below ~200 °C. **I** contained ~8% material with M_n = 540 g/mol and ~92% material with M_n = 1800 g/mol (see **V** later). From a monomodal GPC result, M_n was 1260 g/mol for **I**.

Synthesis of III (M_n = 1730 g/mol)

I (82.9 g, M_n = 1260 g/mol), Et_3N (60 μL), Karstedt's catalyst (40 μL), and allyl glycidyl ether (45 mL, 0.37 mol) were reacted as above. In this way, **III** (88.0 g, 70% yield, T_g = −113 °C, M_w/M_n = 3860/1730 g/mol) was obtained.

^{1}H NMR (δ): [−0.15 (s), −0.13 (s), −0.12 (s), −0.92 (m)] 223H, 0.35 (t, 8H, J = 8 Hz), 1.43 (m, 8H), 2.39 (m, 4H), 2.57 (m, 4H), 2.93 (m, 4H), 3.18 (dd, 4H, J = 5.5 and 5.5), 3.25 (m, 8H), 3.49 (dd, 4H, J = 9 and 2.5 Hz) ppm. ^{13}C NMR (δ): 0.106, 1.03, 1.15, 14.19, 23.51, 44.14, 50.80, 71.45, 74.30 ppm. ^{29}Si NMR (δ): [−22.29, −22.02, −21.49, −18.60] 42Si, 7.57 (s, 4Si) ppm. IR (ν): no Si—H band.

In TGA (N_2), **III** lost 95% of its weight between 200 and 700 °C. In TGA (air), **III** lost 5% of its weight below 175 °C and 65% between 175 and 550 °C.

Preparation of V (M_n = 1800 g/mol)

The lower molecular weight material (6.3 g or ~8%) was removed from **I** (82 g, M_n = 1260 g/mol) as above. In this way, **V** (75.2 g, T_g = −129 °C, M_w/M_n = 3630/1800 g/mol) was isolated.

^{1}H NMR (δ): [−0.016 (s), 0.042 (s), 0.055 (s)] 350H, 0.127 (s, 28H), 4.65 (m, 4H) ppm. ^{13}C NMR (δ): 1.16 ppm. ^{29}Si NMR (δ): [−21.88, −21.82, −21.43, −19.79, −18.48] 41Si; −6.85 (m, 4Si) ppm. IR (ν): 2129 (Si—H) cm^{-1}.

In TGA (N_2), **V** lost 95% of its weight between 175 and 650 °C. In TGA (air), **V** lost 80% of its weight between 125 and 600 °C. Lower molecular weight material removed from **I** (M_n = 1260 g/mol) had M_w/M_n = 580/540 g/mol.

IR (ν): 2128 (Si—H) cm^{-1}.

Preparation of VII (M_n = 1635 g/mol)

V (M_n = 1800, 72.7 g), Et_3N (50 μL), Karstedt's catalyst (30 μL), and allyl glycidyl ether (36 mL, 0.30 mol) were reacted as above. In this way, **VII** (69.8 g, 65% yield, T_g = −115 °C, M_w/M_n = 3450/1635 g/mol) was obtained.

^{1}H NMR (δ): [−0.21 (s), −0.19 (s), −0.093 (s), −0.068 (s), 0.023 (s)] 220H, 0.37 (t, 8H, J = 9 Hz), 1.45 (m, 8H), 2.45 (m, 4H), 2.64 (m, 4H), 2.99 (m, 4H), 3.23 (m, 4H), 3.29 (m, 8H), 3.54 (dd, 4H, J = 8.0 and 3.5 Hz) ppm. ^{13}C NMR (δ): 0.154, 1.10, 1.22, 14.20, 23.53, 44.32, 50.91, 71.49, 74.39 ppm. ^{29}Si NMR (δ): [−22.11, −21.98, −21.70, −21.44, −18.57] 50Si, 7.61 (m, 4Si) ppm. IR (ν): no Si—H band.

In TGA (N_2), **V** lost 95% of its weight between 225 and 700 °C. In TGA (air), **VII** lost 60% of its weight between 200 and 550 °C.

Synthesis of II (M_n = 5780 g/mol)

D_3^F (200 g, 0.43 mol), tetra-SiH (4.61 g, 0.014 mol), and triflic acid (70 μL) were reacted as above. In this way, **II** [193.2 g, 94% yield, T_g = −74 °C, M_w/M_n (bimodal) = 10,420/7350 and 1075/1055 g/mol] was obtained.

^{1}H NMR (δ): [−0.033 (s), 0.012 (s), 0.045 (s)] 456H, 0.61 (m, 279H), 1.88 (m, 279H), 4.56 (m, 4H) g/mol. ^{13}C NMR (δ): −1.02 (m), 9.15, 27.41 (q, J_{C-F} = 30 Hz), 127.36 (q, J_{C-F} = 275 Hz) ppm. ^{19}F NMR (δ): −69.73 (m, 1F), −69.59 (m, 1F) ppm. ^{29}Si NMR (δ): [−23.93 (m), −23.63 (m), −23.46 (m), −23.11 (m), −22.40 (s), −21.19 (s)] 135Si; −5.57 (m, 4Si) ppm. IR (ν): 2133 (Si—H) cm^{-1}.

For TGA (N_2), see Figure 3. In TGA (air), **II** lost ~25% of its weight between 150 and 250 °C. A further 70% weight loss occurred between 375 and 525 °C. **II** contained ~25% material with M_n = 1055 g/mol and ~75% material with M_n = 7350 g/mol (see **VI** later). This gave an average M_n value of 5780 g/mol.

Synthesis of IV (M_n = 3200 g/mol)

II (M_n = 5780 g/mol, 64.8 g), Et_3N (50 μL), Karstedt's catalyst (35 μL), and allyl glycidyl ether (2.5 mL, 0.021 mol) were reacted as above. In this way, **IV** [47.1 g, 70% yield, T_g = −77 °C, M_w/M_n (bimodal) = 6890/5780 and 1115/1090 g/mol] was obtained.

^{1}H NMR (δ): [−0.06 (s), 0.118 (s), 0.175 (m), 0.30 (s)] 444H, 0.38 (t, 8H, J = 8.5 Hz), 0.79 (m, 271H), 1.60 (m, 8H), 2.06 (m, 271H), 2.60 (m, 4H), 2.79 (m, 4H), 3.14 (m, 34H), 3.37 (dd, 4H, J = 6.0 and 5.5), 3.46 (m, 8H), 3.71 (m, 2H), 3.73 (m, 2H) ppm. ^{13}C NMR (δ): −1.08 (m), 8.92 (m), 27.87 (q, J_{C-F} = 30 Hz), 127.57 (q, J_{C-F} = 275 Hz) ppm. ^{19}F NMR (δ): −69.46 (m, 2F), −69.28 (m, 1F) ppm. ^{29}Si NMR (δ): [−23.90, −23.43, −23.38, −23.09 (m), −21.40,

−21.37, −21.14, −21.08, −21.02] 149Si; 9.19 (m, 4Si) ppm. IR (ν): no Si—H band.

For TGA (N_2), see Figure 3. In TGA (air), **IV** lost 60% of its weight below 175 °C. A further 30% weight loss occurred between 200 and 575 °C. On the basis of GPC and TGA (N_2) results, **IV** contained ~55% material with M_n = 1090 g/mol and ~45% material with M_n = 5780 g/mol. This gave an average M_n value of 3200 g/mol.

Preparation of VI (M_n = 5850 g/mol)

The lower molecular weight material (18.8 g, ~25%) was removed from **II** (M_n = 5780 g/mol, 75.9 g) via bulb-to-bulb distillation at 190 °C/0.005 mm. In this way, **VI** (57.1 g, T_g = −74 °C, M_w/M_n = 10,515/5850 g/mol) was isolated.

^{1}H NMR (δ): 0.295 (m, 380H), 0.91 (m, 239H), 2.18 (m, 239H), 4.88 (m, 4H) ppm. ^{13}C NMR (δ): −2.50, −2.19, 8.34, 8.57, 27.42 (q, J_{C-F} = 30 Hz), 127.32 (q, J_{C-F} = 275 Hz) ppm. ^{19}F NMR (δ): −69.50 ppm. ^{29}Si NMR (δ): [−23.49, −23.29 (m), −22.58] 117Si; 5.77 (m, 4Si) ppm. IR (ν): 2132 (Si—H) cm^{-1}.

For TGA (N_2), see Figure 3. In TGA (air), **VI** lost 70% of its weight between 250 and 450 °C. Lower molecular weight material removed from **II** had T_g = −75 °C and M_w/M_n = 1110/1090 g/mol.

IR (ν): 2124 (Si—H) cm^{-1}.

Synthesis of VIII (M_n = 3800 g/mol)

VI (M_n = 5850 g/mol, 54.4 g), Et_3N (40 μL), Karstedt's catalyst (40 μL), and allyl glycidyl ether (10.5 mL, 0.09 mol) were reacted as above. In this way, **VIII** [53.7 g, 83% yield, T_g = −77 °C, M_w/M_n (bimodal) = 7330/5690 and 970/950 g/mol] was obtained.

^{1}H NMR (δ): [−0.06 (s), −0.008 (s), 0.009 (s)] 337H, 0.41 (t, 8H, J = 9 Hz), 0.61 (m, 205H), 1.43 (m, 8H), 1.90 (m, 205H), 2.43 (m, 4H), 2.63 (m, 4H), 2.97 (m, 4H), 3.20 (dd, 4H, J = 6.0 and 5.5 Hz), 3.29 (m, 8H), 3.54 (d, 4H, J = 11 Hz) ppm. ^{13}C NMR (δ): −1.11 (m), 8.98 (m), 14.13 (s), 23.49 (s), 27.87 (q, J_{C-F} = 30 Hz), 71.62, 74.07, 127.34 (q, J_{C-F} = 275 Hz) ppm. ^{19}F NMR (δ): −69.61 (m, 1F), −69.40 (m, 1F) ppm. ^{29}Si NMR (δ): [−23.84 (m), −23.55 (m), −23.18 (m), −23.10 (s), −23.06 (s), −22.98 (s), −22.94 (s), −21.32 (s), −21.28 (s), −21.05 (s), −21.00 (s), −20.92 (s)] 156Si; 9.32 (m, 4Si) ppm. IR (ν): no Si—H band.

For TGA (N_2), see Figure 3. In TGA (air), **VIII** lost 45% of its weight between 130 and 225 °C. A further 40% loss occurred between 250 and 505 °C. On the basis of the GPC and TGA (N_2) results, **VIII** contained ~40% material with M_n = 950 and ~60% material with M_n = 5690 g/mol. This gave an average M_n value of 3800 g/mol.

Synthesis of II (M_n = 1700 g/mol)

D_3^F (150.4 g, 0.32 mol), tetra-SiH (19.2 g, 0.06 mol), and triflic acid (90 μL) were reacted as above. In this way, **II** [168.9 g, 99% yield, T_g = −79 °C, M_w/M_n (bimodal) = 2070/2010 and 1190/1175 g/mol] was obtained.

^{1}H NMR (δ): [0.235 (s), 0.292 (s), 0.327 (s)] 95H, 0.90 (m, 44H), 2.17 (m, 44H), 4.87 (4H) ppm. ^{13}C NMR (δ): 1.98, 2.28, 3.71, 12.39 (m), 12.79, 13.00, 31.83 (q, J_{C-F} = 30 Hz), 131.73 (q, J_{C-F} = 279 Hz) ppm. ^{19}F NMR (δ): −65.79 (m) ppm. ^{29}Si NMR (δ): [−23.67 (m), −23.38 (m), −23.25 (m), −23.11 (m), −22.35 (m), −21.07 (m), −20.42 (bm)] 17Si, [−6.34, −5.99, −5.77, −5.53 (m), −3.81 (m), −2.95 (m)] 4Si ppm. IR (ν): 2127 (Si—H) cm^{-1}.

In TGA (N_2), **II** lost 95% of its weight between 125 and 500 °C. In TGA (air), **II** lost 85% of its weight between 115 and 500 °C. **II** contained ~37% material with M_n = 1175 g/mol and ~63% material with M_n = 2010 g/mol (see **VI** later). This gave an average M_n value of 1700 g/mol.

Synthesis of IV (M_n = 1400 g/mol)

II (M_n = 1700 g/mol, 80 g), Et_3N (65 μL), Karstedt's catalyst (50 μL), and allyl glycidyl ether (15.5 mL, 0.12 mol) were reacted as above. In this way, **IV** (77.7 g, 81% yield, T_g = −84 °C, M_w/M_n = 1780/1400 g/mol) was obtained.

^{1}H NMR (δ): [0.01 (s), 0.10 (s), 0.11 (m), 0.14 (s), 0.16 (s)] 138H, 0.57 (t, 8H, J = 8.5 Hz), 0.77 (m, 63H), 1.61 (m, 8H), 2.04 (m, 63H), 2.58 (m, 4H), 2.76 (m, 4H), 3.12 (m, 4H), 3.36 (q, 4H, J = 5.5), 3.45 (m, 8H), 3.70 (m, 4H) ppm. ^{13}C NMR (δ): −1.33 (m), 8.89 (m), 14.07 (s), 23.47 (s), 23.94 (s), 27.96 (q, J_{C-F} = 30 Hz), 44.22, 50.89, 71.71, 74.21, 127.59 (q, J_{C-F} = 275 Hz) ppm. ^{19}F NMR (δ): −69.40 (m) ppm. ^{29}Si NMR (δ): [−24.45 (m), −24.05 (m), −23.88 (m), −23.66, −23.51 (m), −23.16 (m), −22.90 (m), −21.28, −20.99, −20.92, −20.06 (m)] 23Si, [8.10, 8.74, 8.99, 9.10, 9.19 (m)] 4Si ppm. IR (ν): no Si—H band.

In TGA (N_2), **IV** lost ~100% of its weight between 110 and 500 °C. In TGA (air), **IV** lost 85% of its weight between 100 and 550 °C.

Preparation of VI (M_n = 2040 g/mol)

The lower molecular weight material (37.1 g, ~37%) was removed from **II** (M_n = 1700 g/mol, 99.4 g) as above. In this way, **VI** [60.2 g, T_g = −92 °C, M_w/M_n = 2260/2040 g/mol] was isolated.

^{1}H NMR (δ): [0.19 (s), 0.28 (s), 0.32 (s)] 83H, 0.90 (m, 41H, 2.16 (m, 41H), 4.88 (4H) ppm. ^{13}C NMR (δ): −1.00 (m), 0.40, 9.05, 9.19, 27.95 (q, J_{C-F} = 30 Hz), 127.44 (q, J_{C-F} = 280 Hz) ppm. ^{19}F NMR (δ): −69.54 (m) ppm. ^{29}Si NMR (δ): [−23.14 (m), −22.34, −20.38 (bm)] 19Si, [−5.51, −3.44 (bm)] 4Si ppm. IR (ν): 2129 (Si—H) cm^{-1}.

In TGA (N_2), **VI** lost ~100% of its weight between 200 and 525 °C. In TGA (air), **VI** lost 80% of its weight between 200 and 600 °C. Lower molecular weight material removed from **II** had M_w/M_n = 1155/1125 g/mol and T_g = −98 °C.

IR (ν): 2133 (Si—H) cm^{-1}.

Synthesis of VIII (M_n = 1300 g/mol)

VI (M_n = 2040 g/mol, 56.4 g), Et_3N (45 μL), Karstedt's catalyst (35 μL), and allyl glycidyl ether (13.9 mL, 0.12 mol) were reacted as above. In this way, **VIII** (59.2 g, 85% yield, T_g = −80 °C, M_w/M_n = 1630/1300 g/mol) was obtained.

^{1}H NMR (δ): [0.105 (s), 0.16 (s), 0.17 (s)] 103H, 0.58 (t, 8H, J = 8.5 Hz), 0.77 (m, 49H), 1.60 (m, 8H), 2.05 (m, 49H), 2.59 (m, 4H), 2.78 (m, 4H), 3.13 (m, 4H), 3.36 (m, 4H), 3.45 (m, 8H), 3.71 (m, 4H) ppm. ^{13}C NMR (δ): −1.06 (m), −0.023 (m), 8.92 (m), 14.10 (s), 23.49 (s), 27.86 (q, J_{C-F} = 30 Hz), 44.21 (m), 50.92 (s), 71.60 (m), 74.05 (m), 127.48 (q, J_{C-F} = 275 Hz) ppm. ^{19}F NMR (δ): −69.58 (m) ppm. ^{29}Si NMR (δ): [−22.82 (bm), −20.55, −20.51, −20.28, −20.22, −20.14] 48Si, [8.90, 9.56, 9.58 (m), 9.97, 9.99, 10.04 (m)] 4Si ppm. IR (ν): no Si—H band.

In TGA, **VIII** decomposed between 110 and 500 °C with 98% (N_2) and 85 (air) weight losses.

DISCUSSION

Synthesis of I–VIII

The properties of **I–VIII** are reported in Table 1. The preparation of Si—H-terminated star oligosiloxane (**I**) and star oligofluorosiloxane (**II**) was via the acid-catalyzed equilibration of D_4 and D_3^F with tetra-SiH, respectively (Fig. 1).[31] Cyclosiloxanes can be converted to linear polymers by acid-catalyzed equilibration with a suitable disiloxane.[43] The molecular weights of **I** and **II** were controlled by the ratio of tetra-SiH to D_4 or D_3^F, respectively.

Table 1. Properties of the Star Oligomers (**I–VIII**)

Star Polymer	M_n (g/mol)	m [average degree of polymerization ($\overline{DP}$)]	Low-Molecular-Weight Material (%)	T_g (°C)
Siloxanes				
I (higher molecular weight)	2800	8	9	−127
III	3265	8	5	−119
V	3700	11	0	−127
VII	3600	10	0	−118
I (lower molecular weight)	1260	3	8	−130
III	1730	3	8	−113
V	1800	3	0	−129
VII	1635	3	0	−115
Fluorosiloxanes				
II (higher molecular weight)	5780	9	25	−74
IV	3200	4	55	−77
VI	5850	9	0	−74
VIII	3800	5	40	−77
II (lower molecular weight)	1700	2	37	−79
IV	1400	1	—	−84
VI	2040	3	0	−92
VIII	1300	1	—	−80

Equilibration reactions generate a mixture of linear and cyclic species.[43] Thus, higher molecular weight materials **V** and **VI** were isolated by bulb-to-bulb distillation of lower molecular weight material from **I** and **II**, respectively. Less lower molecular weight material was present in star oligosiloxanes (**I**) versus star oligofluorosiloxanes (**II**). Bulky substituents on silicon are known to drive the equilibrium toward cyclics.[43] The removal of the lower molecular weight material from **V** and **VI** was confirmed by GPC and by the absence of low-temperature weight loss during TGA (N_2). A Si—H band ($\sim$2130 cm^{-1}) was observed in the IR spectra of lower molecular weight materials.

Reactive epoxy groups were readily introduced by the Pt-catalyzed hydrosilylation of **I**, **II**, **V**, and **VI** with allyl glycidyl ether.[30] At the same time, the Si—H groups of the lower molecular weight material present in **I** and **II** were also converted to epoxide groups. A small amount of Et_3N was added to the reaction mixture to prevent ring opening of the epoxide by acidic impurities.

Molecular Weight of I–VIII

Hydrosilylation of star oligofluorosiloxanes (**II** and **VI**) with allyl glycidyl ether resulted in a significant reduction (18–45%) in the molecular weight of the products (**IV** and **VIII**; Fig. 3). For instance, during TGA (N_2), **II** (M_n = 5780 g/mol) experienced a 25% loss in weight between 135 and 260 °C. However, **IV** experienced $\sim$55% weight loss below 175 °C. Thus, **IV** was determined to have an average M_n value of 3200 g/mol (45% decrease). The hydrosilylation of **II** and **VI** at room temperature gave similar results. It is unclear why this reduction in the molecular weight occurred. By GPC and TGA, the hydrosilylation of star oligosiloxanes (**I** and **V**) did not produce similar reductions in the molecular weights of the products (**III** and **VII**; Fig. 3).

T_g's of I–VIII

The T_g's of poly(dimethylsiloxane) and polymethyl(3,3,3-trifluoropropylsiloxane) (PMTFPS) are −123 and −70 °C, respectively.[44] The higher T_g of PMTFPS can be attributed to the electronic repulsion of adjacent CF_3 groups, which causes the propyl groups to become rigid and restrict backbone rotation.[45] The T_g's of **I**, **III**, **V**, and **VII** were −130 to −113 °C, whereas the T_g's of **II**, **IV**, **VI**, and **VIII** were −92 to −74 °C (Table 1).

The T_g's of siloxane **I** with M_n = 2800 g/mol (−127 °C) and siloxane **I** with M_n = 1260 g/mol (−130 °C) were quite similar. After hydrosilylation with allyl glycidyl ether, the T_g's of resulting **III** with M_n = 3265 g/mol (−119 °C) and **III** with M_n = 1730 (−113 °C) were higher. The T_g's of **V** with M_n = 3700 g/mol (−127 °C) and **V** with M_n = 1800 g/mol (−129 °C) were nearly identical. Similarly, the hydrosilylation of these with allyl glycidyl ether produced **VII** (T_g = −118 °C) and **VII** (T_g = −115 °C) with higher T_g's.

The T_g's of the higher molecular weight star fluorosiloxanes (**II**, **IV**, **VI**, and **VIII**) were between −77 and −74 °C. However, the T_g's of the lower molecular weight fluorosiloxanes were lower (−92 to −79 °C). T_g increased with increasing M_n before approaching a constant value.[46]

Thermal Stability of I–VIII

As expected, degradation in air began at lower temperatures than in N_2. The removal of the lower molecular weight material from **I** and **II** to isolate **V** or **VI**, respectively, was marked by an increase in the thermal stability (Fig. 3). The modification of the Si—H terminal groups of star oligosiloxanes **I** and **V** with glycidyloxypropyl groups to yield **III** and **VII**, respectively, produced an enhancement in the thermal stability. However, a similar modification of star oligofluorosiloxanes **II** and **VI** decreased M_n of **IV** and **VIII** (Table 1) and thereby diminished the thermal stability. Fluorosiloxanes typically have lower thermal stability than comparable siloxanes.[47]

Film Preparation

The formation of crosslinked films of **IIIa–IIIc**, **IVa** and **IVb**, **VIIa–VIIc**, and **VIIIa** and **VIIIb** is shown in Figure 2. The formation of fluorosiloxane films was limited. Attempts to prepare films of **IVb** and **IVc** (at higher molecular weights of **IV**), **VIIIb** and **VIIIc** (at higher molecular weights of **VIII**), **IVc** (at lower molecular weights of **IV**), and **VIIIc** (at lower molecular weights of **VIII**) failed to produce films. Thus, only **a** consistently gave films with star oligofluorosiloxanes (**IV** and **VIII**).

On microscope slides, the thickness of the siloxane films (**IIIa–IIIc** and **VIIa–VIIc**) and fluorosiloxane films (**IVa**, **IVb**, **VIIIa**, and **VIIIb**) was $\sim$0.55 and $\sim$0.30 mm, respectively. The film thickness was $\sim$0.1–0.2 mm on aluminum coupons.

Table 2. Properties of the Films

Film	T_g (°C)	T_β (°C)	θ_{static} (°)	θ_{adv} (°)	θ_{rec} (°)	θ_Δ (°)
Siloxane films based on **I** (M_n = 2800 g/mol)						
IIIa	−113	—	121	113	72	41
IIIb	−112	—	109	108	81	27
IIIc	−115	—	119	112	74	38
VIIa	−113	—	128	115	82	33
VIIb	−112	—	116	116	90	26
VIIc	−114	—	114	114	89	25
Siloxane films based on **I** (M_n = 1260 g/mol)						
IIIa	−102	—	113	112	89	24
IIIb	−105	—	111	112	84	28
IIIc	−112	—	112	108	77	31
VIIa	−99	—	114	115	92	23
VIIb	−106	—	108	110	87	23
VIIc	−113	—	107	104	69	35
Fluorosiloxane films based on **II** (M_n = 5780 g/mol)						
IVa	−31	—	99	104	88	16
VIIIa	−41	—	102	110	91	19
Fluorosiloxane films based on **II** (M_n = 1700 g/mol)						
IVa	−39	—	109	114	84	23
IVb	−62	−109	117	113	84	23
VIIIa	−35	—	104	113	100	13
VIIIb	−65	−108	108	110	103	7

T_g's of the Films

The properties of the films are listed in Table 2. For siloxane films based on **I** (M_n = 2800 g/mol), T_g's were quite similar (−115 to −113 °C). The T_g's of fluorosiloxane films based on **II** (−65 to −31 °C) were higher than those of siloxane films based on **I** (−115 to −99 °C).

For fluorosiloxane films based on **II** (M_n = 5780 g/mol), **IVa** (lower molecular weight material present) had T_g = −31 °C. However, the corresponding film of **VIIIa** (lower molecular weight material removed) had T_g = −41 °C. The higher T_g of **IVa** may have resulted from its higher crosslink density. No Si—H band was observed in **IV**. Thus, Si—H terminal groups of lower molecular weight material were also modified with epoxy groups and could participate in subsequent cure reactions with **a** to form a more highly crosslinked film of **IVa** with a higher T_g.[48,49]

Unique properties were observed for some fluorosiloxane films based on **II** (M_n = 1700 g/mol). A β-transition temperature (T_β) was observed for **IVb** (T_β = −109 °C, T_g = −62 °C) and **VIIIb** (T_β = −108 °C, T_g = −65 °C). The loss modulus exhibits a maximum at T_g and at T_β.[50] T_β is typically associated with side-chain mobility.[51] Because a T_β was not observed for other fluorosiloxane films, those noted for **IVb** and **VIIIb** were perhaps due to uncrosslinked ends rather than 3′,3′,3′-trifluoropropyl pendant groups. An imbalance in the stoichiometry of glycidyloxy groups (**IV** and **VIII**) and amine groups (**b**) may have produced uncrosslinked, dangling ends, which resulted in films (**IVb** and **VIIIb**) with lower crosslink density and lower T_g's.[48,49]

G′ of the Network Films

G' is related to the stiffness or resistance to deformation. G' of the films was dependent on the molecular weight of **a**–**c**. G' increased with the crosslink density in the order of **c** < **b** < **a** for most films (Fig. 4).

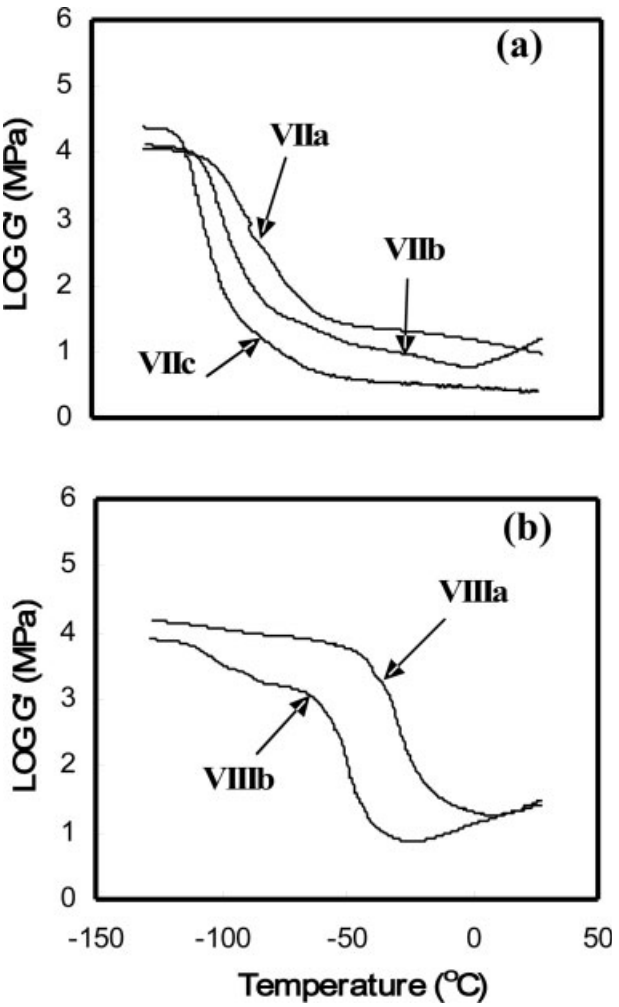

Figure 4. G' of films: (a) **VIIa**–**VIIc** (based on **I**, M_n = 1260 g/mol) and (b) **VIIIa** and **VIIIb** (based on **II**, M_n = 1700 g/mol).

Contact Angles of the Films

The values of θ_{static}, θ_{adv}, and θ_{rec} of distilled/deionized water droplets on the film–air interface are reported in Table 2. For all films, θ_{static} was greater than 90 °C, indicating that they were hydrophobic.[52] Crosslinked siloxane films exhibit exceptional hydrophobicity because the highly flexible siloxane backbones permit the orientation of available methyl groups to the surface.[24] Higher crosslink density decreases backbone flexibility. Thus, more flexible (i.e., lower T_g) siloxane films are anticipated to have lower γ values (i.e., higher contact angle with water). The high θ_{static} values of siloxane films of **IIIa–IIIc** and **VIIa–VIIc** (107–128°) were consistent with their low T_g's (−115 to −99 °C). Because of the higher surface activities of CF_3— groups versus CH_3— groups, fluorosiloxane films generally exhibit lower γ values than siloxane films.[29] However, the θ_{static} values for fluorosiloxane films (**IVa** and **IVb** and **VIIIa** and **VIIIb**) were lower (99–117°) than those of siloxane films (**IIIa–IIIc** and **VIIa–VIIc**). This may be attributed to the higher crosslink densities of the fluorosiloxane films, which inhibited the reorganization of CF_3— groups to the surface.

θ_{adv} is an indicator of the hydrophobicity or low surface energy, whereas θ_{rec} reflects the hydrophilic nature of the surface.[53] Hysteresis ($\theta_\Delta = \theta_{adv} - \theta_{rec}$) is a product of surface chemical heterogeneity, roughness, reorganization, hydration, or contamination.[54] θ_Δ is observed for fluoroalkyl pendant groups that undergo surface reorganization.[18] The θ_Δ values of the siloxane films were higher (23–41°) than those of the fluorosiloxane films (7–23°). These dynamic surface tension results may also be attributed to the higher crosslink density of the fluorosiloxane films, which inhibited surface reorganization.

Thermal Stability of the Films

Siloxane films were generally stable to 325 °C, whereas fluorosiloxane films began to degrade at ~200 °C. Fluorosiloxanes have lower thermal stability than comparable siloxanes.[47] The thermal stabilities of the films depended on the molecular weights of **a–c** and increased in the order of **a** < **b** < **c** (Fig. 5).

Bioassays with Ulva Sporelings

Ulva, found throughout the intertidal seashores, is the most predominant ship-fouling macroalga.[5] Spores settled normally, and all nonsettled spores remained motile; this indicated that the leachate was nontoxic. The growth of sporelings on siloxane and fluorosiloxane films was nearly always less than that on the glass standard (Figs. 6 and 7). For siloxane films, the lowest sporeling growth was noted for **IIIa–IIIc** (based on **I**, M_n = 2800 g/mol; Fig. 6). These films displayed relatively low values of G' and T_g (−113 to −115 °C) but higher θ_{static} (119–121°) and θ_Δ (38–41°). The removal of sporelings was greatest from **IIIa** (~49% removed). Siloxane films prepared with α,ω-bis(3-aminopropyl)PDMS **a** (n = 0) generally showed a higher percentage of foul release.

The biomass of *Ulva* sporelings was generally less on the fluorosiloxane films (**IVa**, **IVb**, **VIIIa**, and **VIIIb**) than on the siloxane films (Fig. 7).

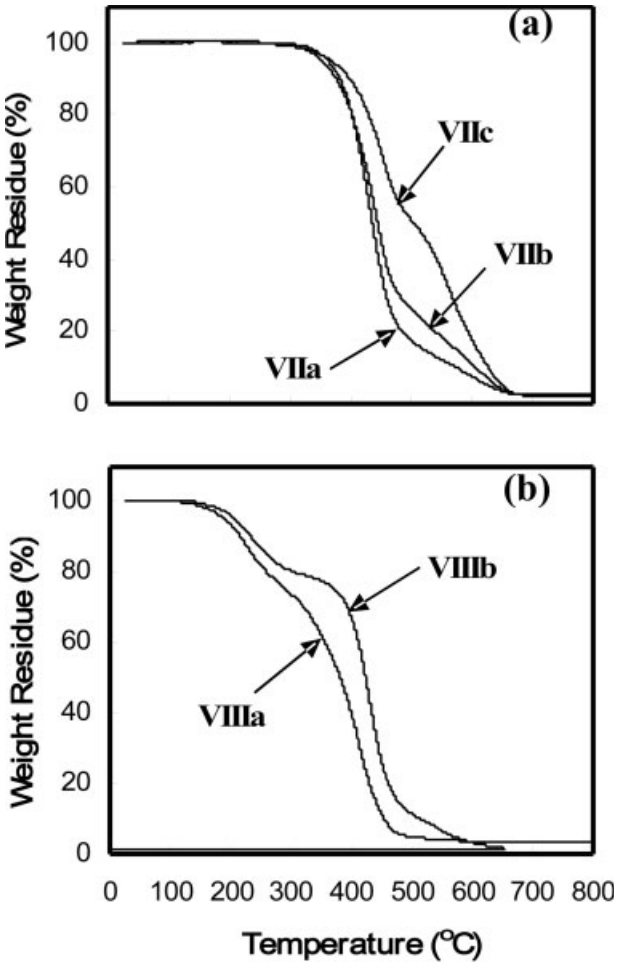

Figure 5. TGA (N_2) of films of (a) **VIIa–VIIc** (based on **I**, M_n = 1260 g/mol) and (b) **VIIIa** and **VIIIb** (based on **II**, M_n = 1700 g/mol).

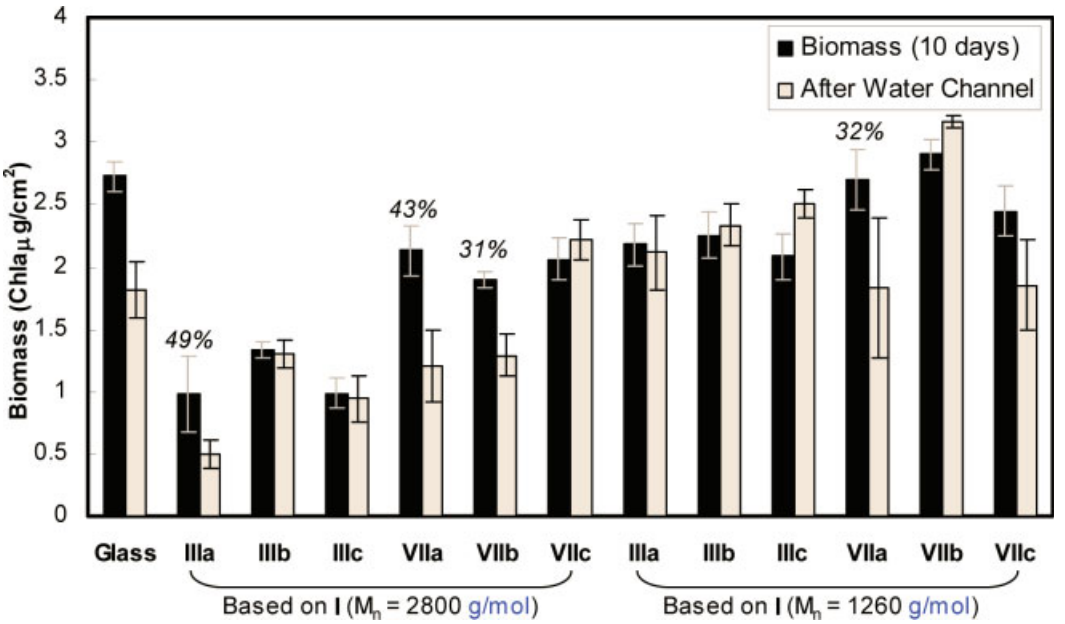

Figure 6. *Ulva* sporeling growth (10 days) and that remaining after exposure to a water channel (shear stress = 53 Pa) on siloxane films.

For fluorosiloxane films, the lowest sporeling biomass was observed on **IVa** (based on **II**, M_n = 5780 g/mol) and **IVa** (based on **II**, M_n = 1700 g/mol). The highest sporeling removal was noted for **IVa** (based on **II**, M_n = 1700 g/mol; ~77% removed). This result is similar to that observed for removal from a commercial siloxane elastomer, Veridian (International Paints).[42] **IVa** had a relatively low T_g (−39 °C) and high θ_Δ (23°) versus other fluorosiloxane films. The removal of sporelings from all other fluorosiloxane films was less than 10%.

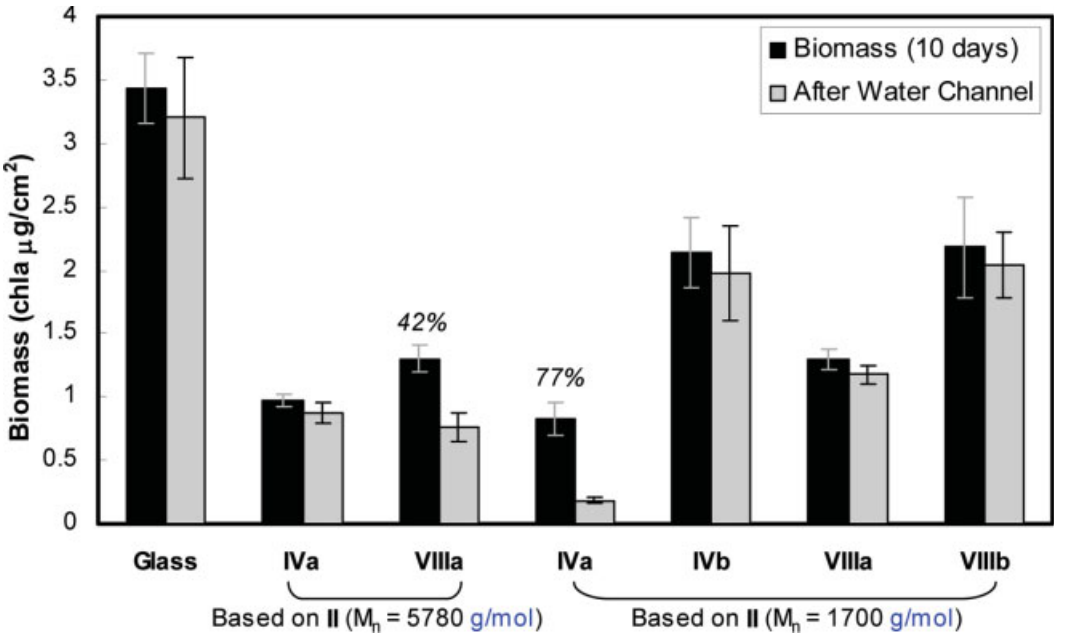

Figure 7. *Ulva* sporeling growth (10 days) and that remaining after exposure to a water channel (shear stress = 53 Pa) on fluorosiloxane films.

Corrosion Protection of Aluminum

Impedance spectra for the coated aluminum (3105 H14 alloy) panels and a bare control panel are shown in Figure 8. The spectra for the control showed the typical pitting behavior observed for aluminum alloys exposed to chloride solutions; a second time constant (due to the contribution from growing pits) was observed in the low-frequency region, and the total capacitance increased with the exposure time [Fig. 8(d)]. The experimental results could be analyzed by means of the PITFIT module of ANALEIS software.[55] The spectra for the aluminum panel coated with a film of **IIIa** agreed with the coating model, which contains contributions from the properties of the (porous) coating and the corrosion reaction of the base metal at the base of the pores in the coating [Fig. 8(a)].[56,57] The pore resistance was quite low and decreased with the exposure time; this indicated increasing porosity with time. Changes in the capacitance of **IIIa** with time could not be observed because the corresponding impedance values were outside the high-frequency limit of the equipment. The spectra for aluminum panels coated with a film of **IIIb** or **IIIc** (based on **I**, M_n = 2800 g/mol) showed capacitive behavior and no significant changes in the impedance values with the exposure time [Fig. 8(b,c)]. Their capacitances did not significantly change during the exposure time, and this indicated that they had little porosity and did not take up significant amounts of water. Impedance spectra for fluorinated films of **IVa**, **IVb**, **VIIIa**, and **VIIIb** showed that the coating capacitance did not change with time. However, their pore resistance was low and decreased with the exposure time. These fluorinated films provided much less corrosion protection than siloxane films (**IIIa**–**IIIc**). Thus, **IIIb** and **IIIc** provided excellent corrosion protection for aluminum samples in 0.5 N NaCl, whereas **IIIa**, **IVa**, **IVb**, **VIIIa**, and **VIIIb** showed various degrees of porosity and increasing degradation over time.

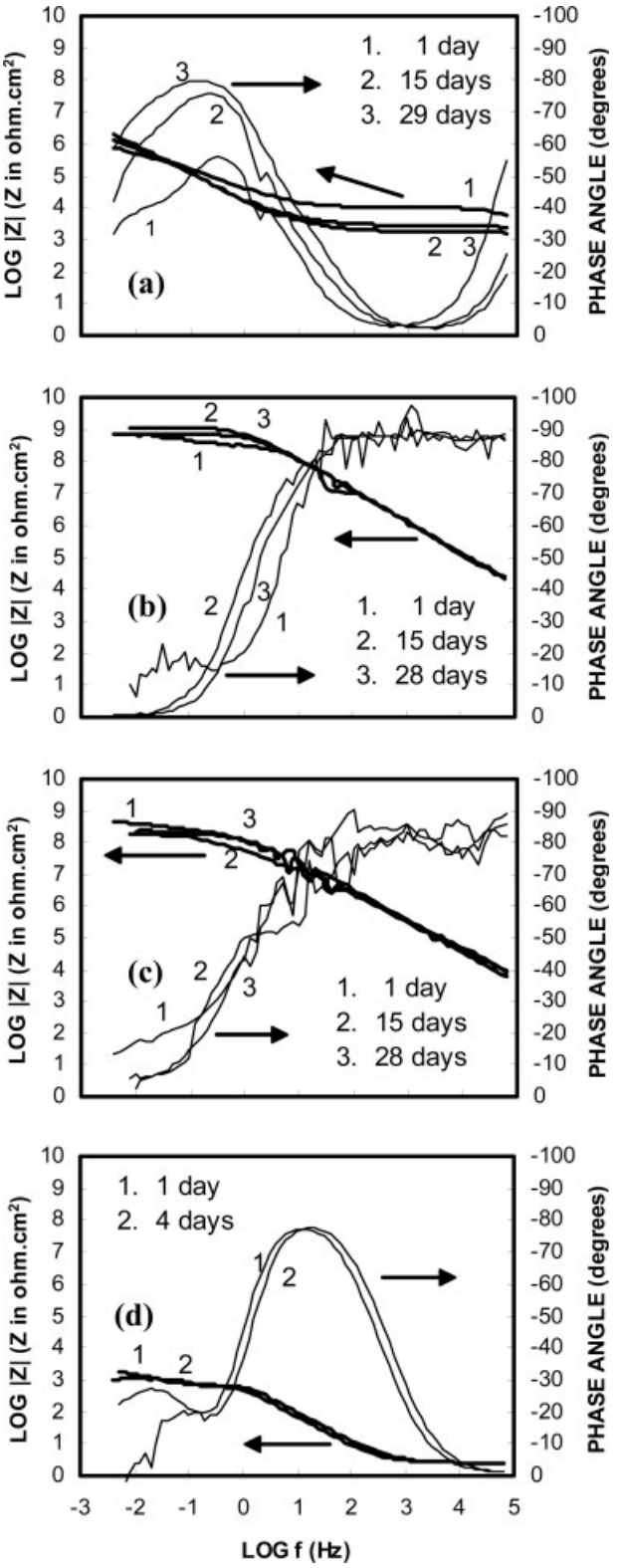

Figure 8. Bode plots for aluminum coupons coated with siloxane films based on **I** (M_n = 2800 g/mol): (a) **IIIa**, (b) **IIIb**, (c) **IIIc**, and (d) a bare aluminum control (f = frequency, $|Z|$ = impedance modulus).

CONCLUSIONS

Epoxy-terminated irregular tetrabranched star oligosiloxanes (**III** and **VII**) and star oligofluorosiloxanes (**IV** and **VIII**) were prepared by the acid-catalyzed equilibration of D_4 or D_3^F and tetrakis (dimethylsiloxy)silane (tetra-SiH) followed by Pt-catalyzed hydrosilylation of allyl glycidyl ether.

Films were generated by the crosslinking of these with an α,ω-bis(3-aminopropyl)PDMS (**a**–**c**). The composition and crosslink density of the films were systematically altered by the variation of the molecular weight of **III**, **IV**, **VII**, and **VIII** and the type of α,ω-bis(3-aminopropyl)PDMS (**a**, **b**, or **c**) incorporated into the film. Siloxane and fluorosiloxane films prepared herein exhibited low γ values (i.e., they were hydrophobic), low G' values, and low T_g values and so are suitable candidates for MAPSs for foul-release coatings.

This work sought to define the relationship between the physical properties of films and their foul-release properties as well as their ability to inhibit corrosion for the future design and synthesis of marine coatings. θ_{static} values were higher for siloxane films of **IIIa**–**IIIc** and **VIIa**–**VIIc** (107–128°) than for fluorosiloxane films of **IVa**, **IVb**, **VIIIa**, and **VIIIb** (99–117°). θ_Δ was also greater for siloxane films (23–41°) than for fluorosiloxane films (7–23°). These results were unexpected because fluorosiloxanes typically have lower γ values. However, the lower molecular weights of star oligofluorosiloxanes (**IV** and **VIII**) led to an increase in their crosslink density versus siloxane films, which likely inhibited the orientation of CF_3 groups to the surface. G' increased with decreasing molecular weight of **III**, **IV**, **VII**, or **VIII** as well as α,ω-bis(3-aminopropyl)PDMS (**a**–**c**). As expected, T_g's of siloxane films (−115 to 99 °C) were lower than those of fluorosiloxane films (−65 to −31 °C). Despite higher values of γ, G', and T_g, the fluorosiloxane films generally exhibited superior foul-release properties with *Ulva* sporelings versus siloxane films. The highest sporeling removal was noted for a fluorosiloxane film of **IVa** (∼77% removed): $T_g = -39$ °C, $\theta_{static} = 109°$, and $\theta_\Delta = 23°$. These results suggest that these siloxane films, being minimally crosslinked to the extent that their T_g's approached that of linear chains, may have enhanced adhesion of *Ulva* spores, perhaps by penetration of the adhesive into the film. The impedance spectra for coated aluminum (3105 H14 alloy) exposed to 0.5 N NaCl showed that corrosion protection provided by the films of **IIIa**, **IVa**, **IVb**, **VIIIa**, and **VIIIb** was quite poor, whereas excellent results were obtained for films of **IIIb** and **IIIc**.

These findings may provide guidance for the future design and synthesis of antifoul and foul-release marine coatings with enhanced performance. This synthetic methodology would allow the fine tuning of low γ, G', and T_g values required to achieve superior foul-release behavior. Namely, control over the film crosslink density is critical to achieving optimized values. We anticipate that varying the molecular weight of the star oligosiloxanes and star oligofluorosiloxanes as well as the ratio of these and α,ω-bis(3-aminopropyl)PDMS (**a**–**c**) may further enhance the foul-release behavior.

Support from the Office of Naval Research (N00014-02-1-0521 to W. P. Weber and N00014-02-1-0521 to J. A. Callow and M. E. Callow) is acknowledged. The authors thank Robin L. Garrel (University of California at Los Angeles) for the use of the First Ten Ångstroms FTÅ 4000.

REFERENCES AND NOTES

1. Brady, R. F., Jr. Nature 1994, 368, 16.
2. Bullock, S.; Johnston, E. E.; Wilson, T.; Gatenholm, P.; Wynne, K. J. J Colloid Interface Sci 1999, 210, 18.
3. Omae, I. Chem Rev 2003, 103, 3431.
4. Brady, R. F., Jr. J Coat Technol 2000, 72, 900.
5. Callow, M. E.; Callow, J. A. Biologist 2002, 49, 1.
6. Brady, R. F., Jr. J Prot Coat Linings 2000, 15, 73.
7. Swain, G. W. J.; Schultz, M. P. Biofouling 1996, 10, 187.
8. Kohl, J. G.; Singer, I. L. Prog Org Coat 1999, 36, 15.
9. Uilk, J.; Bullock, S.; Johnston, E.; Myers, S. A.; Merwin, L.; Wynne, K. J. Macromolecules 2000, 33, 8791.
10. Pike, J. K.; Ho, T.; Wynne, K. J. Chem Mater 1996, 8, 856.
11. Schmidt, D. L.; Coburn, C. E.; DeKoven, B. M.; Potter, G. E., Meyers, G. F.; Fischer, D. A. Nature 1994, 368, 39.
12. Wang, J.; Mao, G.; Ober, C. K.; Kramer, E. J. Macromolecules 1997, 30, 1906.
13. Gan, D.; Mueller, A.; Wooley, K. L. J Polym Sci Part A: Polym Chem 2003, 41, 3531.
14. Gudipati, C. S.; Greenlief, C. M.; Johnson, J. A.; Prayongpan, P.; Wooley, K. L. J Polym Sci Part A: Polym Chem 2004, 42, 6193.
15. Grunlan, M. A.; Lee, N. S.; Cai, G.; Gädda, T.; Mabry, J. M.; Mansfeld, F.; Kus, E.; Wendt, D. E.; Kowalke, G. L.; Finlay, J. A.; Callow, J. A.; Callow, M. E.; Weber, W. P. Chem Mater 2004, 16, 2433.
16. Johnston, E.; Bullock, S.; Uilk, J.; Gatenholm, P.; Wynne, K. J. Macromolecules 1999, 32, 8173.
17. Mera, A. E.; Goodwin, M.; Pike, J. K.; Wynne, K. J. Polymer 1999, 40, 419.
18. Uilk, J.; Johnston, E. E.; Bullock, S.; Wynne, K. J. Macromol Chem Phys 2002, 203, 1506.
19. Brady, R. F., Jr. Prog Org Coat 1999, 35, 31.

20. Kinloch, A. J.; Young, R. J. Fracture Behavior of Polymers; Applied Science: London, 1983.
21. Kendall, J. K. Phys D: Appl Phys 1971, 4, 1186.
22. Newby, B. Z.; Chaudhury, M. K.; Brown, H. R. Science 1995, 269, 1407.
23. Wynne, K. J.; Swain, G. W.; Fox, R. B.; Bullock, S.; Ulik, J. Biofouling 2000, 16, 277.
24. Owen, M. J. In Silicon-Based Polymer Science: A Comprehensive Resource; Zeigler, J. M.; Fearon, F. W. G., Eds.; ACS Symposium Series 223; American Chemical Society: Washington, DC, 1990; pp 709–717.
25. Lu, P.; Paulasaari, J. K.; Weber, W. P. Macromolecules 1996, 25, 5561.
26. Paulasaari, J. K.; Weber, W. P. Macromolecules 2001, 33, 1005.
27. Miravet, J. F.; Fréchet, J. M. J. Macromolecules 1998, 37, 3193.
28. Gong, C.; Fréchet, J. M. J. J Polym Sci Part A: Polym Chem 2000, 38, 2970.
29. Owen, M. J. J Appl Polym Sci 1988, 35, 895.
30. Grunlan, M. A.; Lee, N. S.; Weber, W. P. Polymer 2004, 45, 2517.
31. Cai, G.; Weber, W. P. Polymer 2004, 45, 2941.
32. Crivello, J. V.; Bi, D. J Polym Sci Part A: Polym Chem 1993, 31, 3109.
33. Vorderbruggen, M. A.; Crivello, J. V.; Wu, K.; Breneman, C. M. Chem Mater 1996, 8, 1106.
34. Grunlan, M. A.; Lee, N. S.; Weber, W. P. J Appl Polym Sci 2004, 94, 203.
35. Chaudhury, M. K.; Finlay, J. A.; Chung, J. Y.; Callow, M. E.; Callow, J. A. Biofouling 2005, 21, 41.
36. Tang, Y.; Finlay, J. A.; Kowalke, G. L.; Meyer, A. E.; Bright, F. V.; Callow, M. E.; Callow, J. A.; Wendt, D. E.; Detty, M. R. Biofouling 2005, 21, 59.
37. Aston, J. G.; Szabz, G. J.; Fink, J. L. J Am Chem Soc 1943, 65, 1135.
38. Callow, M. E.; Callow, J. A.; Pickett-Heapts, J. D.; Wetherbee, R. J Phycol 1997, 33, 938.
39. Finlay, J. A.; Callow, M. E.; Schultz, M. P.; Swain, G. W.; Callow, J. A. Biofouling 2002, 18, 251.
40. Jeffrey, S. W.; Humphrey, G. F. Biochem Physiol Pflanz 1975, 167, 191.
41. Schultz, M. P.; Finaly, J. A.; Callow, M. E.; Callow, J. A. Biofouling 2000, 15, 243.
42. Schultz, M. P.; Finlay, J. A.; Callow, M. E.; Callow, J. A. Biofouling 2003, 19, 17.
43. Semlyen, J. A. In Siloxane Polymers; Clarson, S. J.; Semlyen, J. A., Eds.; PTR Prentice Hall: Englewood Cliffs, NJ, 1993; pp 19–22.
44. Dvornic, P. R. In Silicon-Containing Polymers; Jones, R. G.; Ando, W.; Chojnowski, J., Eds.; Kluwer Academic: Dordrecht, 2000; pp 185–212.
45. Pierce, O. R. Appl Polym Symp 1970, 14, 7.
46. Organic Coatings: Science and Technology; Wicks, Z. W.; Jones, F. N.; Pappas, S. P., Eds.; Wiley: New York, 1994; Vol. II, p 19.
47. Knight, G. J.; Wright, W. W. Br Polym J 1989, 21, 199.
48. Organic Coatings: Science and Technology; Wicks, Z. W.; Jones, F. N.; Pappas, S. P., Eds.; Wiley: New York, 1994; Vol. I, p 38.
49. Stutz, H.; Illers, K.-H.; Mertes, J. J Polym Sci Part B: Polym Phys 1990, 28, 1483.
50. Sperling, L. H. Introduction to Physical Polymer Science, 3rd ed.; Wiley: New York, 2001; p 308.
51. Menard, K. P. Dynamic Mechanical Analysis: A Practical Introduction; CRC: Boca Raton, FL, 1999; p 95.
52. Sangermano, M.; Bongiovanni, R.; Malucelli, G.; Priola, A.; Pollicino, A.; Recca, A. J Appl Polym Sci 2003, 89, 1524.
53. Davies, J.; Nunnerley, C. S.; Brisley, A. C.; Edwards, J. C.; Finalyson, S. D. J Colloid Interface Sci 1996, 182, 437.
54. Johnson, R. E., Jr.; Dettre, R. H. J Phys Chem 1964, 68, 1744.
55. Mansfeld, F.; Shih, H. J Electrochem Soc 1998, 135, 1171.
56. Mansfeld, F. J Appl Electrochem 1995, 25, 187.
57. Kus, E.; Grunlan, Weber, W. P.; Mansfeld, F. J Electrochem Soc B 2005, 152, 236.